Quantum Physics Letters
An International Journal

http://dx.doi.org/10.18576/qpl/060102

Particle Scattering by Quantum Scatterers in Restricted Geometries

Ankita Bhattacharya[1,2] *and Shyamal Biswas*[1,*]

[1] School of Physics, University of Hyderabad, C.R. Rao Road, Gachibowli, Hyderabad-500046, India
[2] Institute of Theoretical Physics, TU Dresden, 01069 Dresden, Germany

Received: 27 Feb. 2017, Revised: 12 Mar. 2017, Accepted: 16 Mar. 2017
Published online: 1 Apr. 2017

Abstract: We have analytically explored the quantum phenomenon of particle scattering by quantum scatterers in restricted geometries. We have considered short ranged (Fermi-Huang δ_p^3 [1]) interactions among the incident particle and the scatterers with no interactions among the scatterers, and the scatterers as (i) particle(s) in a 1-D box, (ii) particles(s) in an array of 1-D boxes, (iii) particle(s) in a 2-D rectangular box, etc. Coherent scattering even by a single boson/fermion in a finite geometry gives rise to rich physics specially for the interference between the scattering due to the aperture and that due to the scatterers in the aperture. We also have explored temperature dependence of differential scattering cross-sections for the above cases with ideal Bose and Fermi scatterers.

Keywords: Quantum scattering, diffraction, unfixed scatterers, box geometries, particles in array of boxes, Bose and Fermi scatterers, temperature dependence of differential scattering cross-section

1 Introduction

In the existing literature, quantum scattering is discussed mostly for classical scatterers which are either fixed in space or having classical motions in space. There is hardly any theoretical discussion on particle scattering by an unfixed quantum scatterer bounded in a region of space except some cases with harmonic oscillators [2,3,4, 5,6,7]. 'Particle'[1] can be scattered coherently from each and every point of a finite region of space of a quantum scatterer if it is fired onto the restricted region (aperture), and can further interfere constructively and destructively with the particle scattering by the aperture. Thus, we naturally take up discussion on quantum scattering, for a wide class of quantum scatters, to introduce quantum scattering with quantized motions of the scatterers in restricted geometries as probe, for the Fermi-Huang δ_p^3 [1] interactions (among the 'incident' particle and the scatterers), which although are easy to deal with have huge applications in the field of ultra-cold atoms [8].

If a plane wave (e^{ikz}) associated with a free particle ('particle') of a fixed momentum ($\mathbf{p} = \hbar k\hat{k}$) is scattered by a fixed scatterer (situated at $\mathbf{r} = 0$) with an interacting

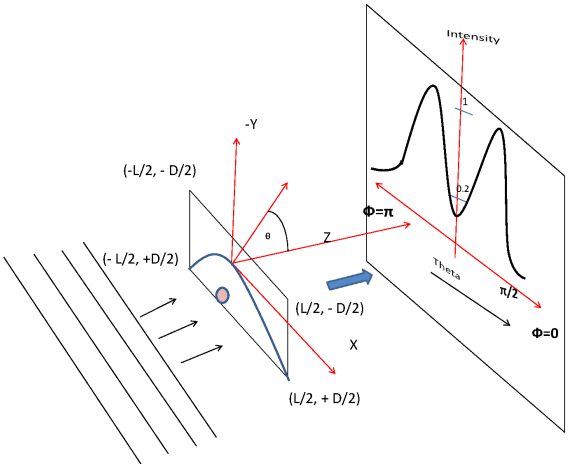

Fig. 1: Intensity distribution, i.e. the total differential scattering cross-section $D_{1,1}(\theta,\phi)$ in units of nm^2, along a line parallel to the x-axis, for scattering of a 'particle' (e^{ikz}) by a quantum scatterer in its ground state in the 2-D box. Plot follows from Eqn.(29) for the parameters $L = 20$ nm, $D = 1$ nm, $kL = 10$, $a_s/L = 0.5$, and $M =$ mass of ^{87}Rb. Direction of the positive x-axis is represented by $\phi = 0$, and that of the negative x-axis is represented by $\phi = \pi$.

[1] Here, by 'particle', we mean, the wave associated with the particle.

* Corresponding author e-mail: sbsp@uohyd.ac.in

potential ($V_{\rm int}(\mathbf{r})$), then spherical wave ($\frac{e^{ikr}}{r}$) goes out of the scatter with a scattering amplitude ($f(\theta,\phi)$) to a particular direction (θ and ϕ) with respect to the initial direction ($\hat{k}$). Now, if the scatterer is not fixed, say, the scatterer is a particle in a 1-D box ($-L/2 < x_0 < L/2$), then the 'particle' would be scattered coherently from all the positions ($\{x_0\}$) with probability density $|\psi_n^{(p)}(x_0)|^2$ where $\psi_n^{(p)}(x_0) = \sqrt{\frac{2}{L}}\cos(\frac{n\pi x_0}{L})$ (for odd $n = 1,3,5...$, and $\sqrt{\frac{2}{L}}\sin(\frac{n\pi x_0}{L})$ for even $n = 2,4,6,...$) is the normalized energy eigenstate of the scatterer. In this situation, spherical waves ($\frac{e^{ikr'}}{r'}$) will go out after scattering form all the source (of scattering) points ($\{x_0\}$). To a particular direction (θ,ϕ) at a distance $\mathbf{r} = \mathbf{x}_0 + \mathbf{r}'$ from the center of the box, all the outgoing spherical waves ($\{\frac{e^{ikr'}}{r'}\}$) interfere with different phases and give rise to coherent scattering amplitude $f_n^{(p)}(\theta,\phi)$ which now depends on the quantum state ($|\psi_n^{(p)}>$) of the scatterer.

This article is organized as follows. In section 2, we have revisited the quantum scattering theory for a classical scatterer, and have calculated the scattering amplitude ($f^{(p)}(\theta,\phi)$) for the Fermi-Huang potential (i.e. regularized δ^3 potential: $V_{\rm int}(\mathbf{r}) = g\delta_p^3(\mathbf{r}) = g\delta^3(\mathbf{r})\frac{\partial}{\partial r}r$). Section 3 has been devoted to the generalization of the quantum scattering theory for quantum scatterers, in particular, for (i) particle(s) in a 1-D box, (ii) particles(s) in an array of 1-D boxes, (ii) particle(s) in a 2-D rectangular box, etc. In the same section, we also have revisited the phenomenon of diffraction of the 'particle' as a problem of quantum scattering specially when it passes through an aperture [9], and have calculated the corresponding aperture scattering amplitude ($f^{(a)}(\theta,\phi)$) for all the above cases. We have calculated the total scattering amplitude $f_n(\theta,\phi) = f_n^{(p)}(\theta,\phi) + f^{(a)}(\theta,\phi)$, and have plotted the total differential scattering cross-section ($D_n(\theta,\phi) = |f_n(\theta,\phi)|^2$) for all the cases. We also have explored temperature dependence of differential scattering cross-sections for the above cases with ideal Bose and Fermi scatterers. Finally, we have summarized our results in the concluding section 4.

2 Quantum scattering for a classical scatterer

In quantum scattering theory, time independent Schrodinger equation is dealt with by the following form of wave function [10]

$$\psi(\mathbf{r}) = \psi(r,\theta,\phi) \simeq A\left[e^{ikz} + f^{(p)}(\theta,\phi)\frac{e^{ikr}}{r}\right], \qquad (1)$$

where the first term represents a incident 'particle', second term represents a outgoing spherical wave in the radiation zone with the scattering amplitude $f^{(p)}(\theta,\phi)$ along a particular direction (θ,ϕ in usual convention) with respect to the initial direction of incidence $\hat{k}$, and $|A|^2$ is proportional to the intensity of the incident 'particle'. Scattering amplitude in Eqn.(1), takes the form, within the first order Born approximation, as [10]

$$f^{(p)}(\theta,\phi) \simeq -\frac{m}{2\pi\hbar^2}\int V_{\rm int}(\mathbf{r}_0)e^{i(\mathbf{k}-\mathbf{k}')\cdot\mathbf{r}_0}d^3\mathbf{r}_0, \qquad (2)$$

where m is the mass of the incident particle, $\mathbf{r}_0$ represents a source of scattering point, $|\mathbf{k}'| = |\mathbf{k}| = k$, and $\mathbf{k}' = k[\sin(\theta)\cos(\phi)\hat{i} + \sin(\theta)\sin(\phi)\hat{j} + \cos(\theta)\hat{k}]$. However, inclusion of all orders of the Born series, modifies Eqn.(2), for the regularized δ^3 (i.e. $V_{\rm int}(\mathbf{r}) = g\delta^3(\mathbf{r})\frac{\partial}{\partial r}r$) potential, as [11,12,8]

$$f^{(p)}(\theta,\phi) = -\frac{mg}{2\pi\hbar^2(1+ik\frac{mg}{2\pi\hbar^2})}, \qquad (3)$$

where the coupling constant (g) can be connected with the s-wave scattering length (a_s) as $g = \frac{2\pi\hbar^2 a_s}{m}$ [8]. In Eqn.(3), we have considered the scatterer to be fixed. If it is not fixed rather having a relative motion, and if the interacting potential still remains the same, then the scattering amplitude would be modified to

$$f^{(p)}(\theta,\phi) = -\frac{\bar{\mu}g}{2\pi\hbar^2(1+ik\frac{\mu g}{2\pi\hbar^2})}, \qquad (4)$$

where $\bar{\mu} = \frac{mM}{m+M}$ is the reduced mass and M is the mass of the scatterer. Eventually, the coupling constant, for this case, would be $g = \frac{2\pi\hbar^2 a_s}{\mu}$ [8].

In Eqn.(4), although we have considered relative motion for the scatterer, yet the scatterer is still classical as we have not quantized motion of the scatterer. Quantum scattering of the 'particle' for (both the first and the second) quantized motions of the scatterers was not surprisingly been studied before for scatterer(s) in a box geometry. In the following section, we are going to study the same for scatterers as (i) particle(s) in a 1-D box, (ii) particles(s) in an array of 1-D boxes, (iii) particle(s) in a 2-D rectangular box, *etc* with further consideration, that, motions of the scatterers are unaltered (which is possible if $\frac{m}{M} \ll 1$ or if $\bar{\mu} \to m$) in the course of scattering.

3 Quantum scattering for quantum scatterers

3.1 Quantum scatterers in a 1-D box

Let M be the mass and $x_0\hat{i}$ be the position of a particle-scatterer in a 1-D box of length L, such that, $-L/2 < x_0 < L/2$. If we quantize ($[\hat{x}_0,\hat{p}_0] = i\hbar\mathbf{1}$) motion of the scatterer, then we get an orthonormal and complete set of quantized energy eigenstates, for the Dirichlet boundary condition, as

$$\psi_n^{(p)}(x_0) = \begin{cases} \sqrt{\frac{2}{L}}\cos(\frac{n\pi x_0}{L}) \text{ for } n = 1,3,5,... \\ \sqrt{\frac{2}{L}}\sin(\frac{n\pi x_0}{L}) \text{ for } n = 2,4,6,... . \end{cases} \qquad (5)$$

Energy eigenvalues corresponding to the states $\{\psi_n^{(p)}(x_0)\}$ are given by $\{E_n = \frac{\pi^2\bar{h}^2n^2}{2ML^2}\}$.

Let us now consider a 'particle', i.e. a plane wave Ae^{ikz} associated with a particle of mass m and momentum $\hbar k\hat{k}$, be incident perpendicularly on the box as well as on the scatterer. In this situation, for $m \ll M$ (or for $\bar{\mu} \to m$), quantized motion of the scatterer will not be altered, rather, the 'particle' will be scattered from all the points $-L/2 < x_0 < L/2$ in the box simultaneously[2] with probability density $\{|\psi_n^{(p)}(x_0)|^2\}$ if $|\psi_n^{(p)}>$ be the initial state of the scatterer. The set-up is similar to that in FIG. 1 except consideration of motion of the quantum scatterer along the y-axis.

3.1.1 Contribution of the particle-scatterer to the quantum scattering

If $\mathbf{r}$ be the position of the incident particle such that, $\mathbf{r} = \mathbf{0}$, the centre of the box, is the origin, then the δ_p^3 interaction, as we have expressed before, between the incident particle at $\mathbf{r}$ and the scatterer at $x_0\hat{i}$, can be expressed as

$$V_{\text{int}}(\mathbf{r}) = g\delta_p^3(\mathbf{r} - x_0\hat{i}). \tag{6}$$

Eqn.(4) can be recast, using Eqn.(6), for this problem, as

$$f^{(p)}(\theta,\phi) = -\frac{mg_k}{2\pi\hbar^2}e^{i(\mathbf{k}-\mathbf{k}')\cdot x_0\hat{i}} = -\frac{mg_k}{2\pi\hbar^2}e^{-i\mathbf{k}'\cdot x_0\hat{i}} \tag{7}$$

where $g_k = \frac{g}{1+ika_s}$. However, the quantum scattering has happened from all the points $-L/2 < x_0 < L/2$ simultaneously with respective probability density $\{|\psi_n^{(p)}(x_0)|^2\}$. Thus, the particle-scattering amplitude for the scatterer in the quantum state $|\psi_n^{(p)}>$, can be written, using Eqns.(5) and (7), as

$$\begin{aligned} f_n^{(p)}(\theta,\phi) &= -\frac{mg_k}{2\pi\hbar^2}\int_{-L/2}^{L/2} e^{-i\mathbf{k}'\cdot x_0\hat{i}}|\psi_n^{(p)}(x_0)|^2 dx_0 \\ &= -\frac{mg_k}{2\pi\hbar^2}\,\text{sinc}(q_xL)\,\frac{1}{1-(\frac{q_xL}{n\pi})^2}, \end{aligned} \tag{8}$$

where $q_x = k\sin(\theta)\cos(\phi)/2$. We are calling it particle-scattering[3] amplitude instead of scattering amplitude, as because, it is the result due to the particle-scatterer only. Eqn.(8) is our desired particle-scattering amplitude for the quantized motion of the scatterer in a 1-D box.

It is also possible to obtain result for the classical scatterer in a 1-D box from the same equation (Eqn.(8)). The scatterer must be fixed for $L \to 0$. Thus, putting $L \to 0$ in Eqn.(8) we get back the same result ($f_n^{(p)}(\theta,\phi) = -\frac{mg_k}{2\pi\hbar^2}$) as that obtained in Eqn.(3) for the classical fixed scatterer.

[2] As because, we are not detecting position of the scatterer.

[3] While particle scattering means scattering of particle(s), particle-scattering means scattering by particle(s).

3.1.2 Contribution of the aperture to the quantum scattering

In the previous subsection, we have considered contribution of the particle-scatterer only to the quantum scattering. But, even an empty box can scatter a 'particle' (wave: Ae^{ikz}) when incident on it, almost like the phenomenon of single slit diffraction.

According to Fresnel-Kirchoff formalism for scalar diffraction, if $\psi_{in} = Ae^{ikz}$ be the scalar field (wave) incident with an angle θ_0 on a plane surface S of an aperture, then due to diffraction through the aperture, the scalar field at the point P far away from the aperture, is given by [9]

$$\begin{aligned} \psi_P &= \frac{-ik}{2\pi}\int_S d\hat{S}\cdot\left(\frac{\hat{k}+\hat{r}'}{2}\right)\frac{e^{ikr'}}{r'}\psi_{in} \\ &= \frac{-ik}{2\pi}\int_S dS\left(\frac{\cos(\theta_0)+\cos(\theta')}{2}\right)\frac{e^{ikr'}}{r'}\psi_{in}, \end{aligned} \tag{9}$$

where $\mathbf{r}'$ is the distance of the point P from an arbitrary point on the surface of the aperture, and θ' is the angle of $\mathbf{r}'$ with the normal $\hat{n}$ of the surface. For normal incidence ($\theta_0 = 0$), and for the Fraunhofer diffraction in the radiation zone, we recast Eqn.(9), as

$$\psi_p \simeq \frac{-ik}{2\pi}A\left(\frac{1+\cos(\theta)}{2}\right)\frac{e^{ikr}}{r}\iint e^{-i(k_xx_0+k_yy_0)}dx_0dy_0 \tag{10}$$

where $\mathbf{r} = \mathbf{r}_0 + \mathbf{r}'$ is the position of the point P from the centre of the surface of the aperture, $\mathbf{r}_0$ is a point on the surface, $r \gg r_0$, $z = 0$ on the surface, x_0 and y_0 are the respectively x and y coordinates of a point on the surface. From Eqn.(9) for we get the aperture-scattering amplitude, comparing with the form of ψ_{out} in Eqn.(1), for a rectangular aperture ($-L/2 < x_0 < L/2$; $-D/2 < y_0 < D/2$) of area $\bar{A} = LD$, as

$$\begin{aligned} f^{(a)}(\theta,\phi) &= \frac{-ik[1+\cos(\theta)]}{4\pi}\int_{-L/2}^{L/2}e^{-ik_xx_0}\int_{-D/2}^{D/2}e^{-ik_yy_0} \\ &= \frac{e^{-i\pi/2}k\bar{A}[1+\cos(\theta)]}{4\pi}\,\text{sinc}(q_xL)\,\text{sinc}(q_yD) \end{aligned} \tag{11}$$

where $q_y = k\sin(\theta)\sin(\phi)/2$. We are calling it aperture-scattering amplitude instead of scattering amplitude, as because, it is the result due to the aperture only.

Eqn.(11) is a result for a 2-D rectangular aperture. We can reach our desired 1-D result from here. To get the result for the 1-D aperture (box) as already mentioned in the previous sub-subsection, we have to put $L/D \ll 1$ and $kD \gg 1$ keeping $A = DL$ nonzero finite constant in Eqn.(11). As $Dk \gg 1$, $\text{sinc}(q_yD) \to 0$, except ($\text{sinc}(q_yD) \to 1$) for two nontrivial cases, we have $\phi = 0$ (+ve x-axis) and $\phi = \pi$ (-ve x-axis). Thus, aperture-scattering amplitude for the 1-D aperture, can be obtained from Eqn.(11), as

$$\begin{aligned} f^{(a)}(\theta,\phi) &= \frac{e^{-i\pi/2}k\bar{A}[1+\cos(\theta)]}{4\pi}\,\text{sinc}(kL\sin(\theta)/2) \\ &\quad\times[\delta_{\phi,0}+\delta_{\phi,\pi}]. \end{aligned} \tag{12}$$

3.1.3 Total scattering amplitude for the quantum scatterer in the 1-D box

Total scattering amplitude for the scatterer in the 1-D box, is given by the superposition of the contributions in Eqns.(8) and (12), as

$$\begin{aligned} f_n(\theta,\phi) &= f_n^{(p)}(\theta,\phi) + f^{(a)}(\theta,\phi) \\ &= -\frac{mg_k}{2\pi\hbar^2}\mathrm{sinc}\left(\frac{kL\sin\theta\cos\phi}{2}\right)\frac{1}{1-\left(\frac{kL\sin\theta\cos\phi}{2\pi n}\right)^2} \\ &\quad -\frac{ik\bar{A}[1+\cos(\theta)]}{4\pi}\mathrm{sinc}\left(\frac{kL\sin\theta}{2}\right)[\delta_{\phi,0}+\delta_{\phi,\pi}] \end{aligned} \quad (13)$$

and the total differential cross-section, as

$$\begin{aligned} D_n(\theta,\phi) &= |f_n(\theta,\phi)|^2 \\ &= \left| a_k \mathrm{sinc}\left(\frac{\pi L\sin\theta\cos\phi}{\lambda}\right)\frac{1}{1-\left(\frac{L\sin\theta\cos\phi}{n\lambda}\right)^2} + \right. \\ &\quad \left. \frac{i\bar{A}[1+\cos(\theta)]}{2\lambda}\mathrm{sinc}\left(\frac{\pi L\sin\theta}{\lambda}\right)[\delta_{\phi,0}+\delta_{\phi,\pi}] \right|^2 \end{aligned} \quad (14)$$

where $a_k = a_s/(1+ika_s)$. Total scattering cross-section, of course, is given by $\sigma_n = \int_{\theta=0}^{\pi}\int_{\phi=0}^{2\pi} D_n(\theta,\phi)\sin(\theta)\mathrm{d}\theta\mathrm{d}\phi$.

It is interesting to note from Eqn.(14), that, the differential scattering cross-section due to the particle and that due to the aperture are comparable if $\bar{A} \sim \lambda|a_s|$ which is possible in nano-length scale, in particular, for quantum dots. In this situation, the diffraction pattern would be greatly modified due to presence of even a single particle in the 1-D box. We plot the total differential cross-section (intensity distribution) in FIG. 2 and in the inset of FIG. 3 for relevant values of parameters for the scatterer(s) in the 1-D box. This intensity distribution is experimentally observable. It is interesting to note, that, the sub-principal maxima in FIG. 3 (inset) is occurring at $n\lambda\sin\theta\cos\phi = L$, specially when integral multiple of the wavelength matches with the length of the 1-D box for the scattering to the perpendicular direction ($\theta = \pi/2,\ \phi = 0,\pi$). From the positions of these maxima in the plot one can determine the energy eigenstate $|\psi_n^{(p)}>$ of the scatterer if occupies a pure state. For forward scattering ($\theta = 0$) and repulsive ($a_s > 0$) or attractive ($a_s < 0$) interactions, height of the peak (or dip along a particular line) of the intensity distribution would be maximum (or minimum) according to the suitable values of a_s, k, and L as already have shown for 2-D box in FIG. 1. The peak (or dip), of course, happens for constructive (or destructive) interference, along some particular directions, between the scattering due to the aperture and that due to the scatterer in the aperture. Thus, just by adjusting wavelength and length of the 1-D box, one can determine s-wave scattering length of the scattered particle.

3.1.4 Temperature dependence of the scattering amplitude

Let us now consider the situation, that, the scatterer in the 1-D box be a subsystem, and it is in thermal equilibrium with its surroundings at temperature T. In this situation, aperture-scattering amplitude $f^{(a)}(\theta,\phi)$ would be unchanged as it is. Modification would be there only in the particle-scattering amplitude part $f_n^{(p)}(\theta,\phi)$. In this situation, the scatterer would be in a mixed state except for $T \to 0$. In the mixed state, the energy eigenstate $|\psi_n^{(p)}>$ has probability $P_n = \frac{\mathrm{e}^{-E_n/k_BT}}{Z}$, where $E_n = \frac{\pi^2\hbar^2n^2}{2ML^2}$, and $Z = \sum_{n=1}^{\infty}\mathrm{e}^{-E_n/k_BT}$ is the canonical partition function. While for $T \to 0$, we have $P_n = \delta_{n,1}$; for $T \to \infty$, we have $P_n =$ constant $\forall n$. However, in thermal equilibrium,

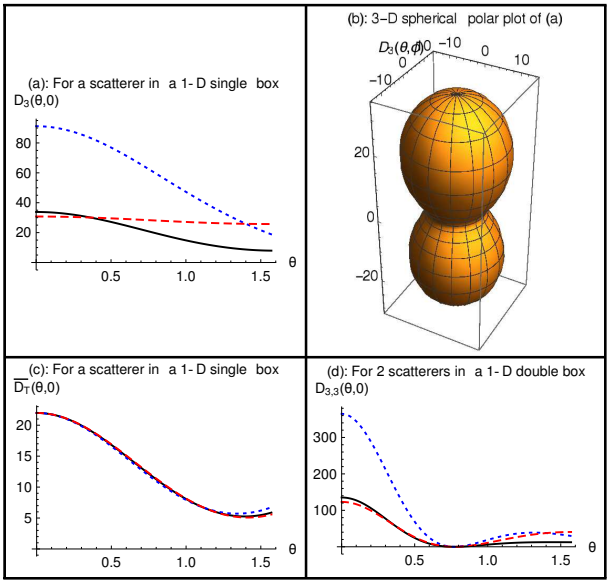

Fig. 2: Total differential scattering cross-section in units of nm^2 for quantum scatterer(s) in 1-D box geometry with the second as 3-D spherical polar plots. For all the figures, we have considered the following: $L = 10$ nm, $kL = 2\pi L/\lambda = 1.5$, $a_s/L = 1$, $\bar{A} = 10\times 40$ nm^2, and $M =$ mass of ^{87}Rb. In FIG 2.(a): the dotted line represents aperture-scattering (diffraction), the dashed line represents particle-scattering, and the solid line, which represents superposition of the two, follows Eqn.(14). FIG 2.(b) represents 3-D spherical polar plot of the case in FIG.2 (a) more with the ϕ dependence. In this figure, the top-face middle point corresponds to $\theta = 0$, and right-face middle point corresponds to $\phi = 0$. Particle-scattering part in the solid, dotted, and dashed lines in the FIG 2.(c) follow from Eqn.(15) for $T = 10^{-2}$K, $T \to 0$, and $T \to \infty$ respectively. In FIG 2.(d): the dotted line represents aperture-scattering, the dashed line represents particle-scattering, and the solid line represents superposition of the two which follow from Eqn.(26) for $\bar{n}_j = \delta_{j,3}$, $N' = 2$ and $b/L = 2$. Vertically upward direction in the figures represents z direction, the horizontal axis (from the left to the right) represents x-axis, and the axis into the page represents the y-axis for the spherical polar plot.

average scattering amplitude, due to the particle, would be

$$\bar{f}_T^{(p)}(\theta,\phi) = \sum_{n=1}^{\infty} f_n^{(p)}(\theta,\phi)P_n$$
$$= -a_k \mathrm{sinc}\left(\frac{\pi L \sin\theta\cos\phi}{\lambda}\right) \sum_{n=1}^{\infty} \frac{P_n}{1-\left(\frac{L\sin\theta\cos\phi}{n\lambda}\right)^2} \quad (15)$$

which, for $T \to 0$, would become

$$\bar{f}_{T\to 0}^{(p)}(\theta,\phi) = -a_k \mathrm{sinc}\left(\frac{\pi L \sin\theta\cos\phi}{\lambda}\right) \frac{1}{1-\left(\frac{L\sin\theta\cos\phi}{\lambda}\right)^2} \quad (16)$$

On the other hand, for $T \to \infty$, scatterer behaves classically, so that, we can conveniently take $n \to \infty$ in Eqn.(8). Thus we can read Eqn.(15), for $T \to \infty$, as

$$\bar{f}_{T\to\infty}^{(p)}(\theta,\phi) = -a_k \,\mathrm{sinc}\left(\frac{\pi L \sin\theta\cos\phi}{\lambda}\right). \quad (17)$$

Eventually, we can replace $f_n^{(p)}(\theta,\phi)$ by $\bar{f}_T^{(p)}(\theta,\phi)$ (as in Eqn.(15)) everywhere, specially in Eqns.(13) and (14), to get the temperature dependence of the average coherent scattering amplitude and that of the differential scattering cross-section respectively.

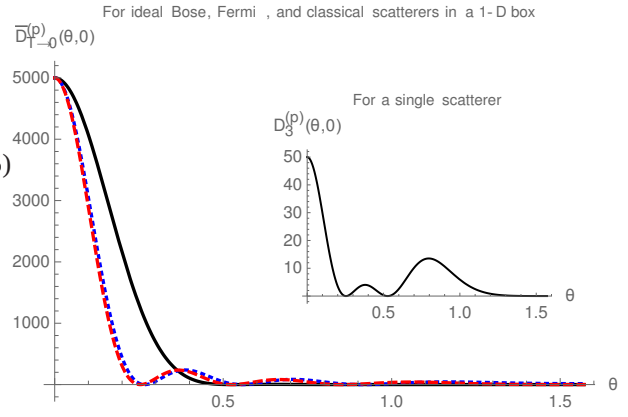

Fig. 3: Particle-scattering part of the differential scattering cross-section in units of nm^2 for $N = 10$ scatterers in 1-D box with other parameters $L = 250$ nm, $kL = 2\pi L/\lambda = 25$, $a_s/L = 0.04$, $\bar{A} = 250 \times \frac{1}{3}$ nm^2 and $M =$ mass of ^{87}Rb. Solid, dotted and dashed lines correspond to Bose, Fermi and classical scatterers, and represent modulus squared of right hand sides of Eqns. (23), (24) and (25) respectively. Inset represents particle scattering part of Eqn.(14) for the same parameters.

3.1.5 Quantum scattering for many quantum scatters in the 1-D box

Let us now consider two noninteracting particle-scatters in the 1-D box, and both of them interact similarly with the incident 'particle' with the interacting potential $V_{\rm int}(\mathbf{r}) = g[\delta_p^3(\mathbf{r}-x_1\hat{i}) + \delta_p^3(\mathbf{r}-x_2\hat{i})]$ where $x_1\hat{i}$ and $x_2\hat{i}$ are positions of the two scatterers in the box. If their positions are fixed, then particle-scattering amplitude, for these two scatterers, can be generalized from Eqn.(7), as

$$f^{(p)}(\theta,\phi) = -\frac{mg_k}{2\pi\hbar^2}[\mathrm{e}^{-i\mathbf{k}'\cdot x_1\hat{i}} + \mathrm{e}^{-i\mathbf{k}'\cdot x_2\hat{i}}]. \quad (18)$$

However, our interest is not in the fixed scatterers, rather in two unfixed quantum scatterers. If the two scatterers are distinguishable, then, their energy eigenstates can be given by

$$\psi_{n,j}^{(p)}(x_1,x_2) = \begin{cases} \frac{2}{L}\cos\left(\frac{n\pi x_1}{L}\right)\cos\left(\frac{j\pi x_2}{L}\right) \text{ for } n,j = \text{odd} \\ \frac{2}{L}\sin\left(\frac{n\pi x_1}{L}\right)\sin\left(\frac{j\pi x_2}{L}\right) \text{ for } n,j = \text{even}, \end{cases} \quad (19)$$

and, for odd n even j, and vice-versa,

$$\psi_{n,j}^{(p)}(x_1,x_2) = \begin{cases} \frac{2}{L}\cos\left(\frac{n\pi x_1}{L}\right)\sin\left(\frac{j\pi x_2}{L}\right) \\ \frac{2}{L}\sin\left(\frac{n\pi x_1}{L}\right)\cos\left(\frac{j\pi x_2}{L}\right). \end{cases} \quad (19a)$$

Thus, contribution of the two distinguishable scatterers to the particle-scattering amplitude would be generalized from Eqn.(8) to

$$f_{n,j}^{(p)}(\theta,\phi) = -\frac{mg_k}{2\pi\hbar^2}\int_{-L/2}^{L/2}\int_{-L/2}^{L/2}[\mathrm{e}^{-i\mathbf{k}'\cdot x_1\hat{i}} + \mathrm{e}^{-i\mathbf{k}'\cdot x_2\hat{i}}]$$
$$\times|\psi_{n,j}^{(p)}(x_1,x_2)|^2 \mathrm{d}x_1\mathrm{d}x_2$$
$$= -\frac{mg_k}{2\pi\hbar^2}\mathrm{sinc}(q_xL)\left[\frac{1}{1-\left(\frac{q_xL}{n\pi}\right)^2} + \frac{1}{1-\left(\frac{q_xL}{j\pi}\right)^2}\right] \quad (20)$$

From Eqn.(20), we can generalize expression of the total differential scattering cross-section in Eqn.(14) for the two distinguishable scatters keeping the aperture scattering part unchanged.

Above expression in Eqn.(20) can be similarly generalized for many (N) identical and distinguishable noninteracting scatterers in the 1-D box, as

$$f_{n_1,n_2,\ldots,n_N}^{(p)}(\theta,\phi) = -\frac{mg_k}{2\pi\hbar^2}\mathrm{sinc}(q_xL)\sum_{j=1}^{N}\frac{1}{1-\left(\frac{q_xL}{n_j\pi}\right)^2}. \quad (21)$$

It is quite natural to expect, that, the expression in Eqn.(21) would be different for N ideal Bose or Fermi scatterers (of same spin component) in the 1-D box. But, it is not the case here. Surprisingly, all the exchange terms in the quantum many scatterers' (bosons or fermions) state ($|\psi_{n_1,n_2,\ldots,n_N}^{(p)}>$) when integrated with the exponentials, like those in Eqn.(20), are zero; e.g. for two Bose or Fermi scatterers an integration with the exchange terms would be $\pm\frac{2^2}{L^2}\int_{-L/2}^{L/2}\mathrm{e}^{-i\mathbf{k}'\cdot x_1\hat{i}}\cos[n\pi x_1/L]\cos[j\pi x_1/L]\mathrm{d}x_1 \times \int_{-L/2}^{L/2}\cos[n\pi x_2/L]\cos[j\pi x_2/L]\mathrm{d}x_2 = 0$, due to orthogonality of the single particle eigenstates for odd $n \neq j$. Thus, Eqn.(21) is also the result of the particle-scattering amplitude, for N Bose or Fermi scatterers, having energy $E_{n_1,n_2,\ldots n_N} = \sum_{j=1}^{N}\frac{\pi^2\hbar^2n_j^2}{2ML^2}$. Eqn.(21) must not be the result for fermions (of the same spin component) if $n_i = n_j$ as $n_i = n_j$ is not allowed for fermions.

However, in thermodynamic equilibrium with a heat and particle bath at temperature T and chemical potential μ, energy distribution is different for different types

(distinguishable, boson, fermion) of scatterers. Thus, particle-scattering amplitude would be different for identical bosons, fermions and distinguishable particles in thermodynamic equilibrium. Average particle-scattering amplitude, for our system of interest, can now be generalized from Eqn.(15), replacing one-scatterer probability by average no. of scatterers $\bar{n}_j$ in single-scatterer state $|\psi_j^{(p)}>$, as

$$\bar{f}_T^{(p)}(\theta,\phi) = \sum_{j=1}^{\infty} \bar{n}_j f_j^{(p)}(\theta,\phi) = -a_k \mathrm{sinc}(\frac{\pi L \sin\theta\cos\phi}{\lambda}) \sum_{j=1}^{\infty} \frac{\bar{n}_j}{1-(\frac{L\sin\theta\cos\phi}{j\lambda})^2}, \quad (22)$$

where $\bar{n}_j = \frac{1}{e^{(E_j-\mu)/k_BT}\mp 1}$ for Bose $(-)$ or Fermi $(+)$ scatterers, and $E_j = \frac{\pi^2\hbar^2 j^2}{2ML^2}$. Interparticle interactions among the scatterers would further perturbatively modify Eqn.(22) for dilute case, and modification can be done by recasting $\bar{n}_j$ keeping its form unaltered within the Hartree-Fock approximation [8,13,14].

However, low and high temperature limits of Eqn.(22) can be easily taken from Eqn.(21). For the Bose scatterers, at $T \to 0$ (and also $\mu \to E_1$ for fixed $\bar{N} = \sum_j \bar{n}_j \to N$), all the scatterers occupy the single-particle ground state ($\bar{n}_1 = N$). Hence, for this case, Eqn.(22) would take the form

$$\bar{f}_{T\to 0}^{(s,b)}(\theta,\phi) = -Na_k \mathrm{sinc}(\frac{\pi L\sin\theta\cos\phi}{\lambda}) \frac{1}{1-(\frac{L\sin\theta\cos\phi}{\lambda})^2} \quad (23)$$

For Fermi scatterers, at $T \to 0$ (and also $\mu = E_F = \frac{\pi^2\hbar^2N^2}{2ML^2}$ for fixed $\bar{N} \to N$), only the first N single-particle states from the ground state onward would be occupied, i.e. $\bar{n}_j = 1$ for $j \le N$ and $\bar{n}_j = 0$ otherwise). Thus, for this case, Eqn.(22) would take the form

$$\begin{aligned}\bar{f}_{T\to 0}^{(s,f)}(\theta,\phi) &= -a_k \mathrm{sinc}(\frac{\pi L\sin\theta\cos\phi}{\lambda}) \sum_{j=1}^{N} \frac{1}{1-(\frac{L\sin\theta\cos\phi}{\lambda j})^2} \\ &= -Na_k \mathrm{sinc}(\frac{\pi L\sin\theta\cos\phi}{\lambda})\Big(1+\frac{1}{2N} \\ &\quad -\frac{L\sin\theta\cos\phi}{2N\lambda}\Big[\pi\cot(\frac{\pi L\sin\theta\cos\phi}{\lambda}) \\ &\quad +h_n(N+\frac{L\sin\theta\cos\phi}{\lambda}) \\ &\quad -h_n(N-\frac{L\sin\theta\cos\phi}{\lambda})\Big]\Big), \end{aligned} \quad (24)$$

where $h_n(x)$ is a harmonic number, and $h_n(N+x)-h_n(N-x)$ vanishes as $1/N$ for large N. On the other hand, for $T \to \infty$, the scatterers behave classically, so that, we can conveniently take the limit $j \to \infty$ in Eqn.(21) as well as in Eqn.(22). Thus, for this case, Eqn.(22) would take the form

$$\bar{f}_{T\to\infty}^{(p,c)}(\theta,\phi) = -Na_k \mathrm{sinc}(\frac{\pi L\sin\theta\cos\phi}{\lambda}). \quad (25)$$

This equation is applicable for identical classical scatterers. Eqns.(23), (24), and (25) clearly say how scattering amplitude is different for different types of scatterers in a 1-D box or single slit. We compare particle-scattering part of the differential cross-section for Bose, Fermi, and classical scatterers in FIG. 3.

Above results can be generalized in the similar spirit for quantum scatterers in many 1-D boxes, e.g. scatterers in a double 1-D box, scatterers in a 1-D grating, *etc* by further considering interference of the outgoing spherical wave coming out of the 1-D boxes. We have shown such a result for two $(1+1)$ scatterers in a 1-D double box in FIG. 2 (d) specially for the spacing (b[4]) of the two 1-D identical boxes as twice of the length an individual box. Temperature dependence of the total differential scattering cross-section for ideal gas of scatterers in N' 1-D identical boxes, in an array with spacing $b = jL$ ($j = 0,1,2,3...$), can be obtained by generalizing Eqns.(14) and (22), as

$$\begin{aligned}\bar{D}_T(\theta,\phi) &= |\bar{f}_T^{(p)}(\theta,\phi) + f^{(a)}(\theta,\phi)|^2 \\ &= \Big| a_k \mathrm{sinc}(\frac{\pi L\sin\theta\cos\phi}{\lambda}) \Big[\sum_{j=1}^{\infty} \frac{\bar{n}_j}{1-(\frac{L\sin\theta\cos\phi}{j\lambda})^2}\Big] \\ &\quad \times \Big[\frac{\sin\left(N'\frac{\pi(b+L)\sin(\theta)\cos(\phi)}{\lambda}\right)}{\sin\left(\frac{\pi(b+L)\sin(\theta)\cos(\phi)}{\lambda}\right)}\Big] \\ &\quad + \frac{i\bar{A}[1+\cos(\theta)]}{2\lambda}\mathrm{sinc}(\frac{\pi L\sin\theta}{\lambda})[\delta_{\phi,0}+\delta_{\phi,\pi}] \\ &\quad \times \Big[\frac{\sin\left(N'\frac{\pi(b+L)\sin(\theta)}{\lambda}\right)}{\sin\left(\frac{\pi(b+L)\sin(\theta)}{\lambda}\right)}\Big]\Big|^2. \end{aligned} \quad (26)$$

Substituting $b = 0$, $N' = 1$ and $\bar{n}_j = \delta_{j,j'}$, we get back Eqn.(14) from the above for a single scatterer in a 1-D box in the state $|\psi_{j'}^{(p)}>$. Substituting $N' = 2$, $\bar{n}_j = \delta_{j,j'}$, we get result for two $(1+1)$ scatterers in a double 1-D box in the state $|\psi_{j',j'}^{(p)}>$.

3.2 Quantum scatterers in a 2-D rectangular box

In the previous subsections we have considered 1-D box (single slit) of length L as a limiting case of a 2-D rectangular box of length L along x-axis and height D along y axis such that $L \ll D$ and $kD \gg 1$ keeping area $\bar{A}$ of the aperture as nonzero finite constant. Let us now consider the general case of the 2-D rectangular box (rectangular aperture) of size $\bar{A} = LD$ and a scatterer in it. The scatterer scatters the incident 'particle' Ae^{ikz}, as stated before, by the interacting potential $V_{\rm int}(\mathbf{r}) = g\delta_p^3(\mathbf{r}-\mathbf{r}_\perp)$, where $\mathbf{r}_\perp = x_0\hat{i}+y_0\hat{j}$ is position of the scatterer in the rectangular aperture such that $-L/2 < x_0 < L/2$ and $-D/2 < y_0 < D/2$.

[4] The spacing is considered from the middle points of the individual boxes.

Particle-scattering amplitude, if the scatterer is fixed at $\mathbf{r} = \mathbf{r}_\perp$, can be generalized from Eqn.(7) as $f^{(p)}(\theta,\phi) = -\frac{mg_k}{2\pi\hbar^2} e^{-i\mathbf{k}'\cdot(x_0\hat{i}+y_0\hat{j})}$. Eigenstate of the scatterer can be written as

$$\psi^{(p)}_{n_x,n_y}(x_0,y_0) = \begin{cases} \sqrt{\frac{2^2}{LD}}\cos(\frac{n_x\pi x_0}{L})\cos(\frac{n_y\pi y_0}{D}) \\ \sqrt{\frac{2^2}{LD}}\sin(\frac{n_x\pi x_0}{L})\sin(\frac{n_y\pi y_0}{D}) \end{cases} \quad (27)$$

for $n_x, n_y = 1,3,5,\ldots$ and $n_x, n_y = 2,4,6,\ldots$ respectively, and

$$\psi^{(p)}_{n_x,n_y}(x_0,y_0) = \begin{cases} \sqrt{\frac{2^2}{LD}}\cos(\frac{n_x\pi x_0}{L})\sin(\frac{n_y\pi y_0}{D}) \\ \sqrt{\frac{2^2}{LD}}\sin(\frac{n_x\pi x_0}{L})\cos(\frac{n_y\pi y_0}{D}) \end{cases} \quad (27a)$$

for the odd-even combination. Energy eigenvalues corresponding to the above states are given by $E_{n_x,n_y} = \frac{\pi^2\hbar^2}{2ML^2}(n_x^2+n_y^2)$. Thus, for the quantized motion of the scatterer, particle-scattering amplitude can now be generalized from Eqn.(8), as

$$\begin{aligned} f^{(p)}_{n_x,n_y}(\theta,\phi) &= -\frac{mg_k}{2\pi\hbar^2}\int_{-L/2}^{L/2}\int_{-D/2}^{D/2} e^{-i\mathbf{k}'\cdot(x_0\hat{i}+y_0\hat{j})} \\ &\quad\times|\psi^{(p)}_{n_x,n_y}(x_0,y_0)|^2 dx_0 dy_0 \\ &= -\frac{mg_k}{2\pi\hbar^2}\frac{\mathrm{sinc}(q_xL)}{1-(\frac{q_xL}{n_x\pi})^2}\frac{\mathrm{sinc}(q_yD)}{1-(\frac{q_yD}{n_y\pi})^2}, \end{aligned} \quad (28)$$

where $q_x = k\sin(\theta)\cos(\phi)/2$ and $q_y = k\sin(\theta)\sin(\phi)/2$ as defined before. Here we see that q_x and q_y parts in the particle-scattering amplitude appear in separable form as motions of the scatterer are independent along x and y direction. On the other hand, aperture-scattering amplitude ($f^{(a)}(\theta,\phi)$), for this case, has already been calculated in Eqn.(11), so that, total differential cross-section can be generalized from Eqn.(14), as

$$\begin{aligned} D_{n_x,n_y}(\theta,\phi) &= |f^{(p)}_{n_x,n_y}(\theta,\phi) + f^{(a)}(\theta,\phi)|^2 \\ &= \Bigg| a_k \frac{\mathrm{sinc}(\frac{\pi L\sin\theta\cos\phi}{\lambda})}{1-(\frac{L\sin\theta\cos\phi}{n_x\lambda})^2}\frac{\mathrm{sinc}(\frac{\pi D\sin\theta\sin\phi}{\lambda})}{1-(\frac{D\sin\theta\sin\phi}{n_y\lambda})^2} \\ &\quad + \frac{i\bar{A}[1+\cos(\theta)]}{2\lambda}\mathrm{sinc}(\frac{\pi L\sin\theta\cos\phi}{\lambda}) \\ &\quad\times\mathrm{sinc}(\frac{\pi D\sin\theta\sin\phi}{\lambda})\Bigg|^2. \end{aligned} \quad (29)$$

We plot the total differential cross-section in FIG. 4 for relevant values of parameters for the scatterer(s) in the 2-D box. We also show that the total forward scattering cross-section $D_{n,m}(0,\phi)$ becomes minimum in FIG. 1 for a different set of parameters. Thus by tuning the set of parameters, e.g. k and L keeping others constant, we can determine the value of s-wave scattering length from the height of the maximum or minimum of the total differential cross-section in the forward direction.

Temperature dependence and other aspects of the total differential scattering cross-section for one and many quantum scatterers in a rectangular aperture can be similarly obtained by multiplying the y dependent part of the scattering amplitude, like that in Eqn.(29), in the right hand sides of Eqns.(15) to (25). Similar generalization is also possible for scatterers in a 2-D double rectangular slits, 2-D grating, etc. We have shown such a result for two $(1+1)$ scatterers in a 2-D double box in FIG. 4 specially for spacing of the two 1-D identical boxes as twice of the length an individual box. Temperature dependence of the total differential scattering cross-sections for 2-D cases can also be obtained in the similar way as prescribed for the 1-D cases.

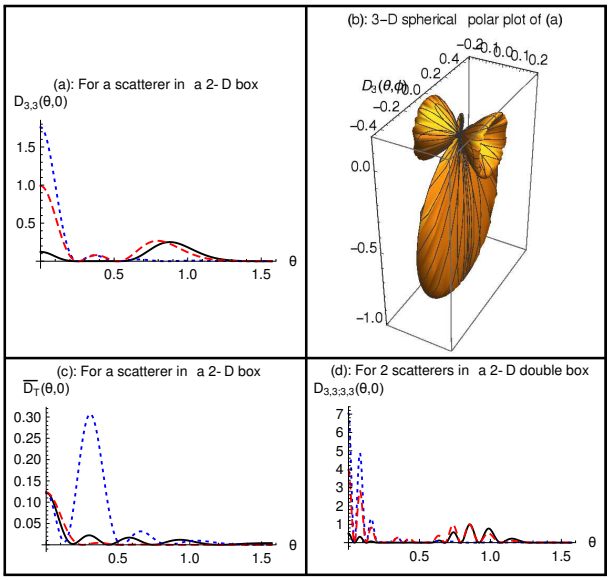

Fig. 4: Total differential scattering cross-section in units of nm^2 for quantum scatterer(s) in 2-D box geometry for the parameters $L = 25$ nm, $D = 1/3$ nm, $kL = 2\pi L/\lambda = 25$, $a_s/L = 0.4$, and $M =$ mass of ^{87}Rb. FIG 4.(a) and (b) follow Eqn.(29). Solid, dotted, and dashed lines in FIG. 4 (c) correspond to $T = 10^{-3}$ K, $T \to 0$, and $T \to \infty$ respectively; and $b/L = 2$ for FIG. 4 (d). All the plots in FIG. 4 correspond to the same plots drawn respectively in FIG. 2.

4 Conclusions

In this article, we have presented a quantum theory of particle scattering for scatterer(s) in quantized bound states in different types of box geometries, e.g. scatterer(s) in a 1-D box, array of 1-D boxes, 2-D rectangular box, etc. Particle scattering by the quantum scatterer(s) in these types of restricted geometries (apertures), which a general reader would find interesting specially for the interference with the scattering by the apertures, has not surprisingly been investigated before. Due to the competition between the aperture-scattering and particle-scattering, usual diffraction pattern can be significantly changed as shown in FIGs. 1, 2, and 4. Due

to the competition, in some situations intensity minimum can appear even for the forward scattering ($\theta = 0$) with $\phi = 0$ or π as shown in FIG. 1, and in some situations, back scattering can dominate over the forward scattering as shown in FIG. 4 (b). From the position of the sub-principal maxima, as shown in FIGs. 3 (inset) and 4 (a), one can determine energy eigenstate of a scatterer in a 1-D or 2-D box, as explained in the last paragraph of the section 3.1.3.

Temperature dependence of differential scattering cross-sections, for ideal gas of Bose and Fermi scatterers in the box geometries, as obtained in Eqn. (22) and shown in FIG. 3, was also not investigated before. Our results on differential scattering cross-section would be important for quantum scattering in nano-length scale, in particular, for particle scattering by quantum dot(s), as also explained in the last paragraph of the section 3.1.3. Temperature dependence of the differential scattering cross-section, on the other hand, would be important within 10^{-2}K to 10^{-3}K as clear from the FIGs. 2 (c) and 4 (c).

All the calculations have been done within the scope of general readers, as because, most of the calculations involve Fourier transformations of the probability amplitudes of the quantum scatterers. Calculations are simple and straightforward, because we did not consider interaction among the quantum scatterers. Simplification also has happened due the Fermi-Huang δ_p^3 [1] interactions (among the 'incident' particle and the scatterers), which although are easy to deal with have huge applications in the field of ultra-cold atoms [8].

General readers can further study quantum scattering for scatterers in harmonically trapped geometry [6] with further consideration of weakly interacting scatterers within perturbation formalism. They can also extend our results on the box geometries for scatterers in other geometries, e.g. circular geometry, cylindrical geometry, etc.

Acknowledgement

A. Bhattacharya acknowledges financial support from the Department of Science and Technology [DST], Govt. of India under the INSPIRE Scholarship Scheme [No. 5495/2011] for an initial part of this work. S. Biswas acknowledges financial support from the DST, Govt. of India under the INSPIRE Faculty Award Scheme [No. IFA-13 PH-70]. We are indebted to C. Timm, TU Dresden, Germany for his valuable critical comments on the work of this article. Useful discussions with S. Dutta Gupta, University of Hyderabad, India are gratefully acknowledged.

References

[1] E. Fermi, Ricerca Sci. **7**, 13 (1936); K. Huang and C. N. Yang, Phys. Rev. **105**, 767 (1957)
[2] Z. Idziaszek, K. Rzazewski, and M. Wilkens, J. Phys. B: At. Mol. Opt. Phys. **32**, L205 (1999)
[3] For experimental data, see, A. P. Chikkatur, A. Gorlitz, D. M. S.-Kurn, S. Inouye, S. Gupta, and W. Ketterle, Phys. Rev. Lett. **85**, 483 (2000)
[4] H.-J. Wang and W. Jhe, Phys. Rev. A **66**, 023610 (2002)
[5] J. Brand, I. Haring, and J.-M. Rost, Phys. Rev. Lett. **91**, 070403 (2003)
[6] A. Bhattacharya and S. Biswas arXiv:1606.02804v3 (2016)
[7] For light scattering by a harmonically trapped BEC, see B. Zhu, J. Cooper, J. Ye, and A. M. Rey, Phys. Rev. A **94**, 023612 (2016)
[8] L. Pitaevskii and S. Stringari, *Bose-Einstein Condensation*, Oxford Sc. Pub. (2003)
[9] S. Dutta Gupta, A. Banerjee, and N. Ghosh, *Wave Optics: Basic Concepts and Contemporary Trends*, Taylor & Francis, New York (2016)
[10] D.J. Griffiths, *Introduction to Quantum Mechanics*, 2nd ed., Pearson Education, Singapore (2005)
[11] C. N. Friedman, J. Functional Analysis **10**, 346 (1972); R. M. Cavalcanti, Rev. Bras. Ens. Fis. **21**, 336 (1999)
[12] I. Mitra, A. DasGupta, and B. Dutta-Roy, Am. J. Phys. **66**, 1101 (1998)
[13] S. Giorgini, L. Pitaevskii, and S. Stringari, Phys. Rev. A **54**, R4633 (1996)
[14] S. Biswas, D. Jana, and R. K. Manna, Eur. Phys. J. D **66**, 217 (2012)

Ankita Bhattacharya obtained M.Sc. degree in Physics from the University of Hyderabad, India in the year 2016. Currently, she is pursuing research for Ph.D. degree at the Institute of Theoretical Physics, TU Dresden, Germany. She works in the field of Condensed Matter Physics (Theory), in particular, Topological Superconductor.

Shyamal Biswas obtained Ph.D. degree in Science from the Indian Association for the Cultivation of Science (*affiliated to* Jadavpur University), Kolkata, India in the year 2009. Then he pursued postdoctoral research in a number of institutes including University of Calcutta (2010-2013) and IIT-Kanpur (May-September, 2013) before joining the School of Physics, University of Hyderabad, India where he is an Assistant Professor now. He works mainly in the field of Statistical and Condensed Matter Physics (Theory), in particular, Quantum Statistical Mechanics.